JYVÄSKYLÄN YLIOPISTO
UNIVERSITY OF JYVÄSKYLÄ

Impact of Octupole Deformation on the Nuclear Electromagnetic Response

8.5.2026

Manu Kanerva, University of Jyväskylä

Markus Kortelainen, University of Jyväskylä

Suomen Akatemia
Finlands Akademi
Research Council of Finland

Centre of Excellence
neutronstars.fi

Octupole deformation and electromagnetic response

- Electromagnetic response
  - Provides a sensitive probe of nuclear structure
  - Collective excitations are sensitive to nuclear deformation
- Reflection-asymmetric (octupole-deformed) shapes are predicted in certain heavy nuclei
  - Strong experimental indications exist for such nuclei
- Octupole deformation breaks intrinsic parity symmetry

→ How does octupole deformation affect electromagnetic response across different multipole modes?

Scope of the study

- Focus on heavy, unstable nuclei with octupole-deformed ground states
  - Even-even isotopes with Z = 86–96 (A = 222–230)
- Electromagnetic response:
  - E1, M1, E2 (IS/IV), E3 (IS/IV)
  - Excitation energy range: 0–38 MeV

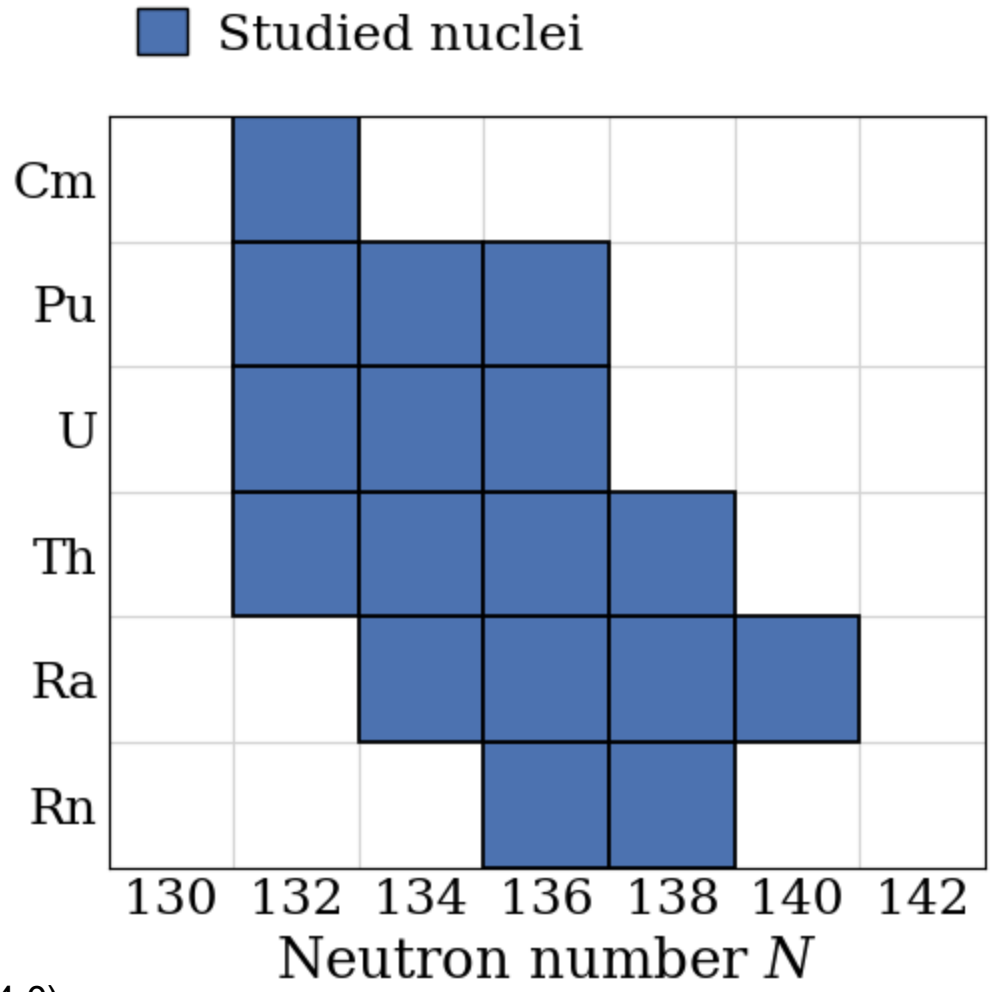

Based on:
M. Kanerva *et al.* Phys. Rev. C 113, 044320 (2026) – DOI: 10.1103/ddl7-y8xj (CC BY 4.0)

Ground states

- Framework: Skyrme–HFB
  - SkM*, SLy4, UNEDF1
- The potential energy surface is explored to identify two distinct ground state solutions:
  - One with conserved reflection symmetry (prolate, $Q_3 = 0$)
  - One with broken reflection symmetry (pear-shaped, $Q_3 \neq 0$)

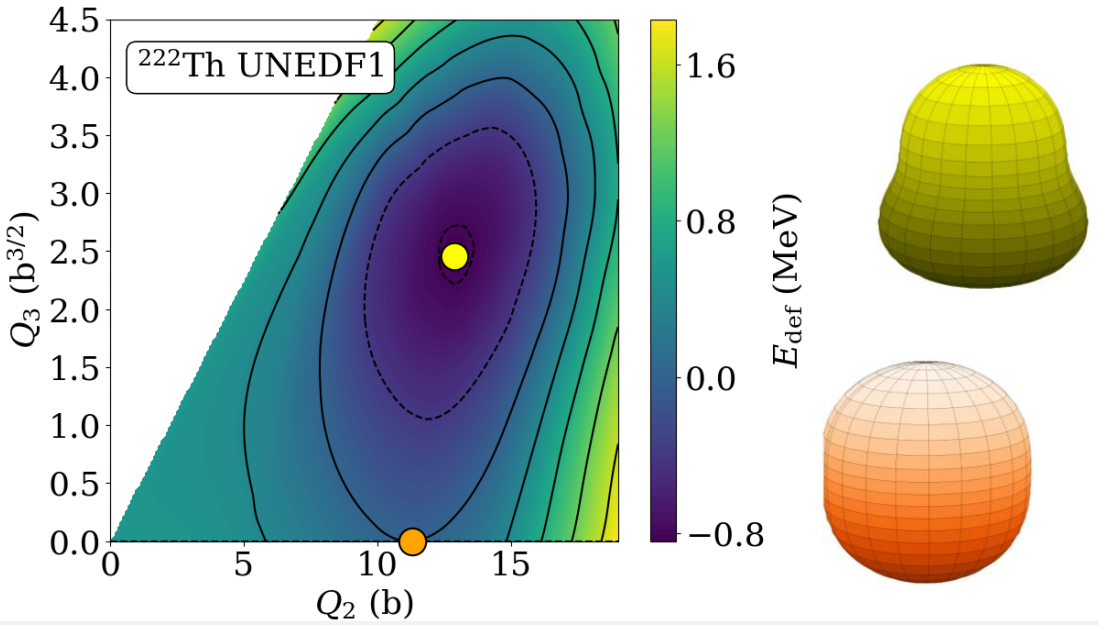

Response to electromagnetic fields

- The obtained ground-state solutions are subjected to a polarizing external field *F*(*t*, *ω*)
  - The linear response of HFB solution is determined by solving the FAM-QRPA equations:

$$(E_k + E_l - \omega)X_{lk}(\omega) + \delta H^{20}_{lk}(\omega) = F^{20}_{lk}(\omega)$$
$$(E_k + E_l + \omega)Y_{lk}(\omega) + \delta H^{02}_{lk}(\omega) = F^{02}_{lk}(\omega)$$

Observables

- Transition strength

$$\frac{dB(\omega,\hat{F})}{d\omega} = \sum_{\mathrm{n}} \left|\langle\Phi_n|\hat{F}(\omega)|\Phi_0\rangle\right|^2 \delta(\omega - E_n)$$
$$= -\frac{1}{\pi}\,\mathrm{Im\ Tr}[f(\omega)(UXV^T + V^*Y^TU^\dagger)]$$

- Photo absorption cross-sections

$$\sigma_{\mathrm{abs}}(\omega) = \frac{4\alpha\pi^2}{\mathrm{e}^2}\,\omega \sum_{K=0,\pm1} \frac{dB(\omega,\hat{F}_{E1}(K))}{d\omega}$$

Electric dipole response

- Photoabsorption cross sections for two Th isotopes (^{222}Th and ^{228}Th) calculated with the SkM* functional
- Differences between the two deformed ground-state solutions are generally small
- A third peak around 16 MeV, prominent in SkM* results, is flattened in some octupole-deformed solutions
  - The suppression is not observed in all isotopes, suggesting that it is not a direct consequence of octupole deformation, but rather induced indirectly

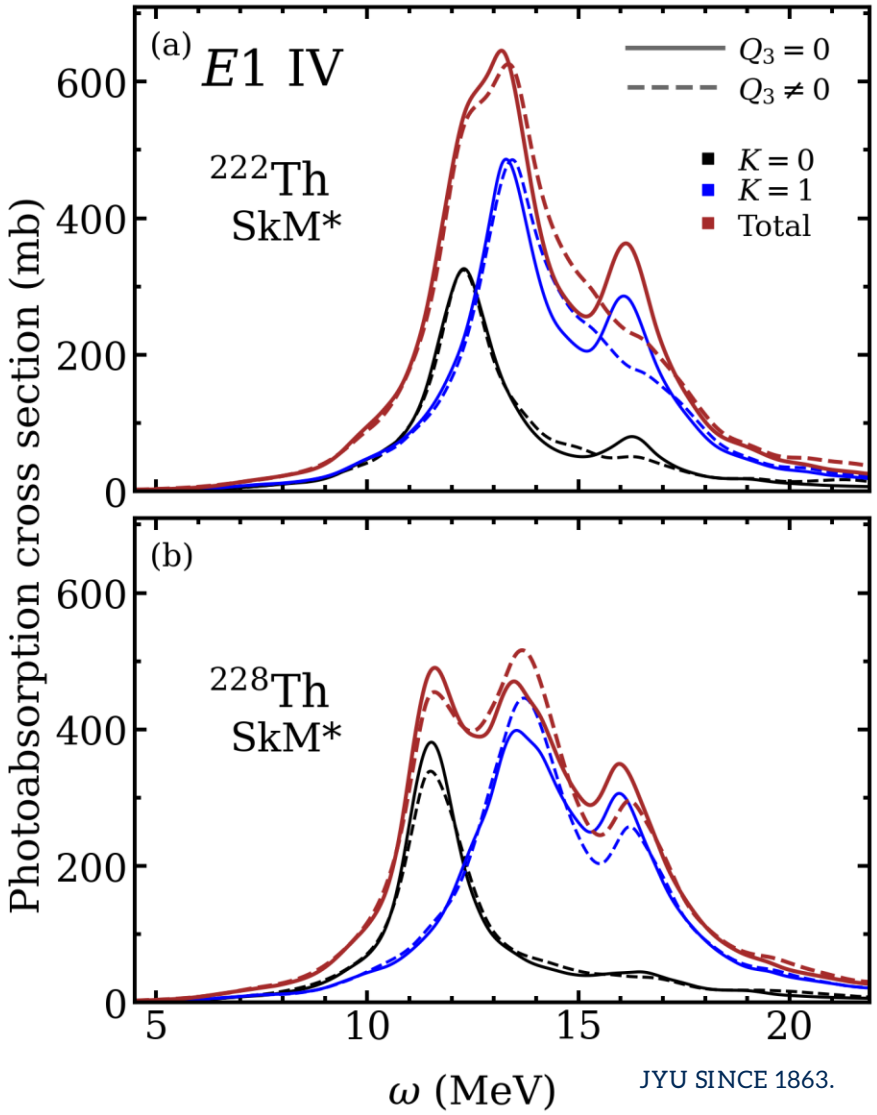

Electric dipole response – functional dependency

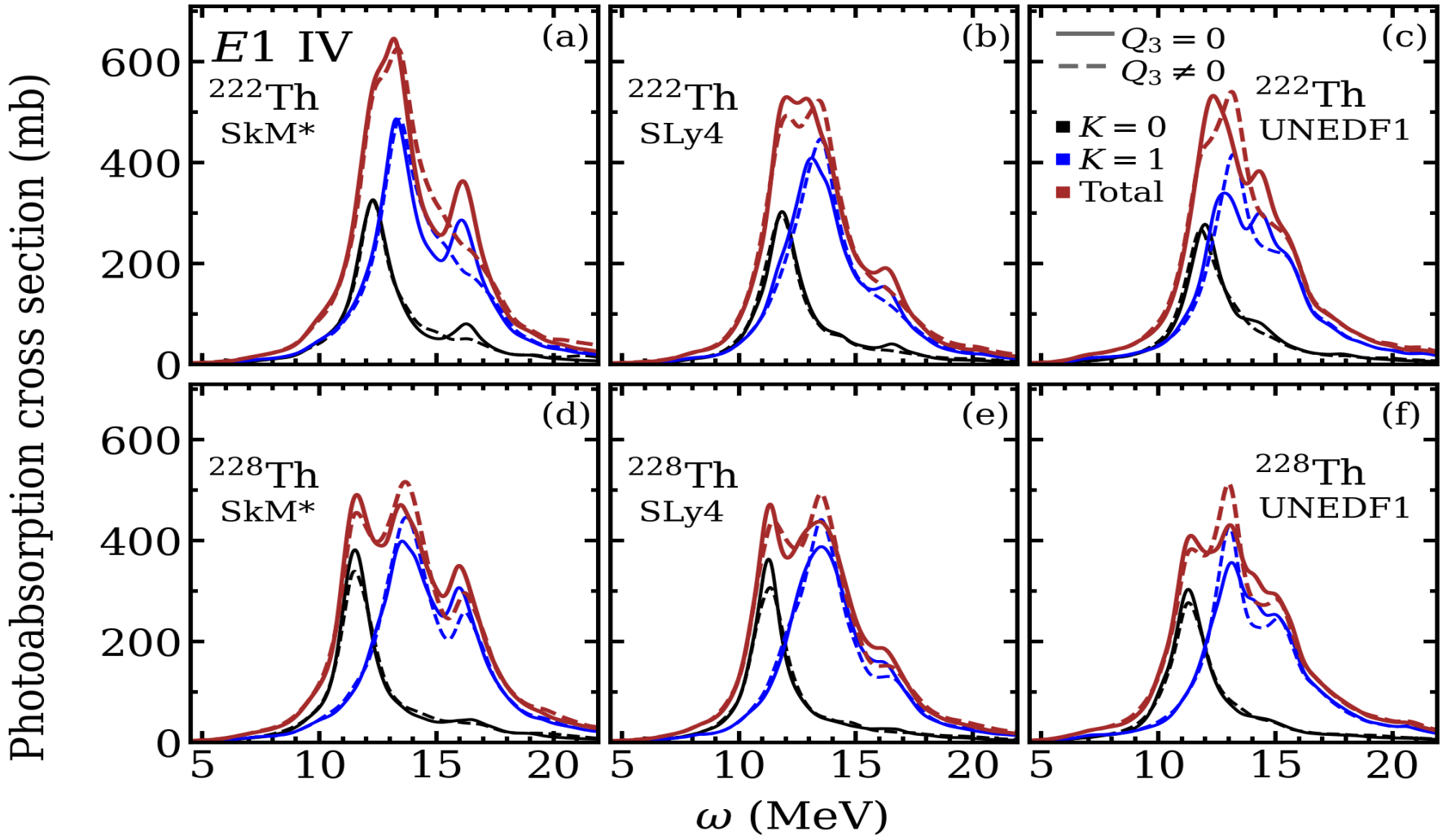

Magnetic dipole response

- $M1$ transition strength functions for three U isotopes (^{224}U, ^{226}U, ^{228}U) calculated with the SkM* and SLy4 functionals
- In the spin-flip region, the transition strength distributions are similar for different deformation minima
- At lower energies, especially around the expected scissors resonance (SR) (~3 MeV), noticeable differences appear between the two deformed ground-state solutions
  - With a smaller smearing width ($\Gamma \approx 2\gamma$), more details can be observed at lower energies

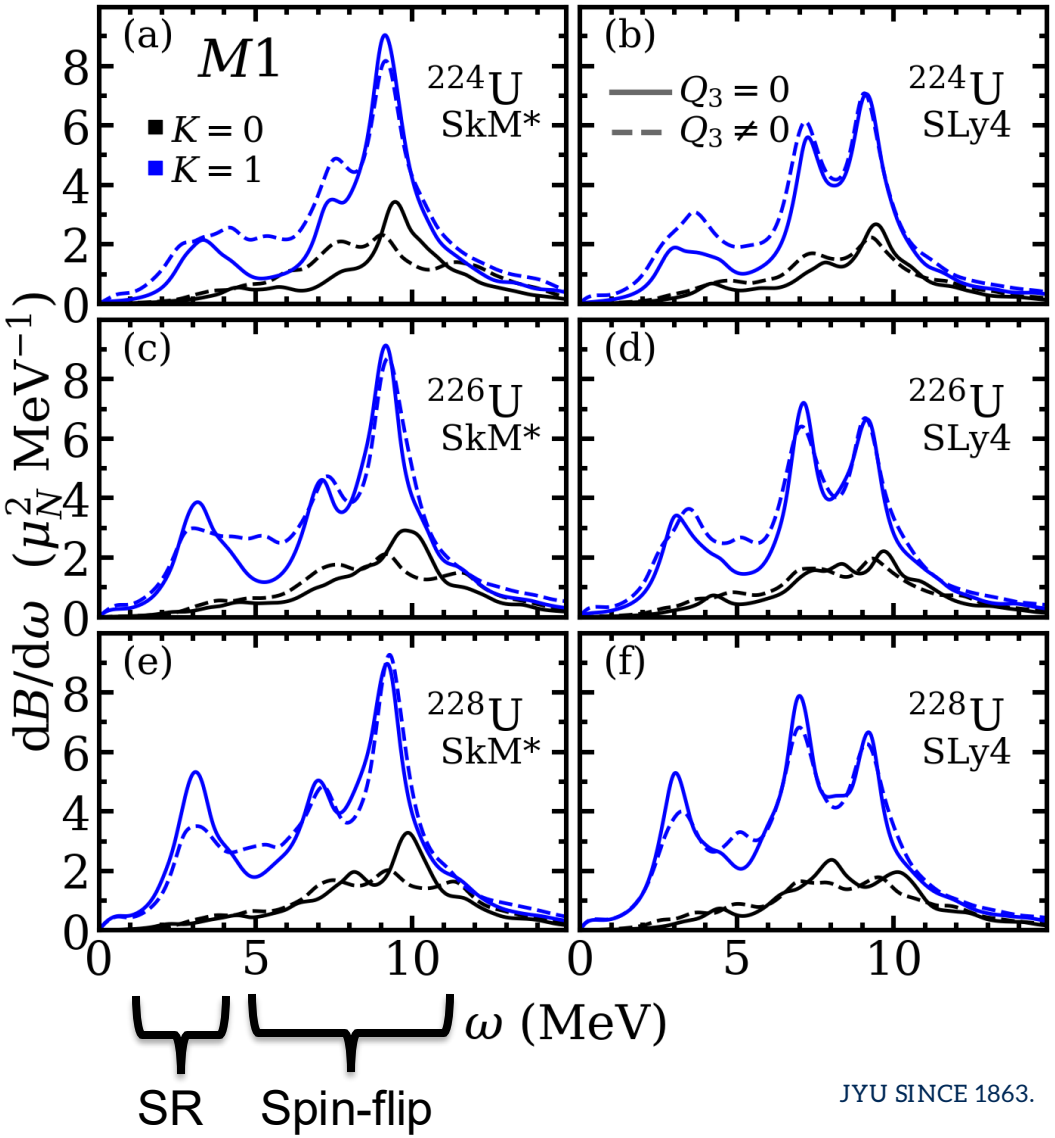

Magnetic dipole response

- *M*1 transition stre
  (^{224}U, ^{226}U, ^{228}U) c
  functionals
- In the spin-flip reg
  distributions are si
  minima
- At lower energies,
  scissors resonance
  differences appear
  ground-state solut
  - With a smaller smearing width ($\Gamma \approx 2\gamma$), more details can be observed at lower energies

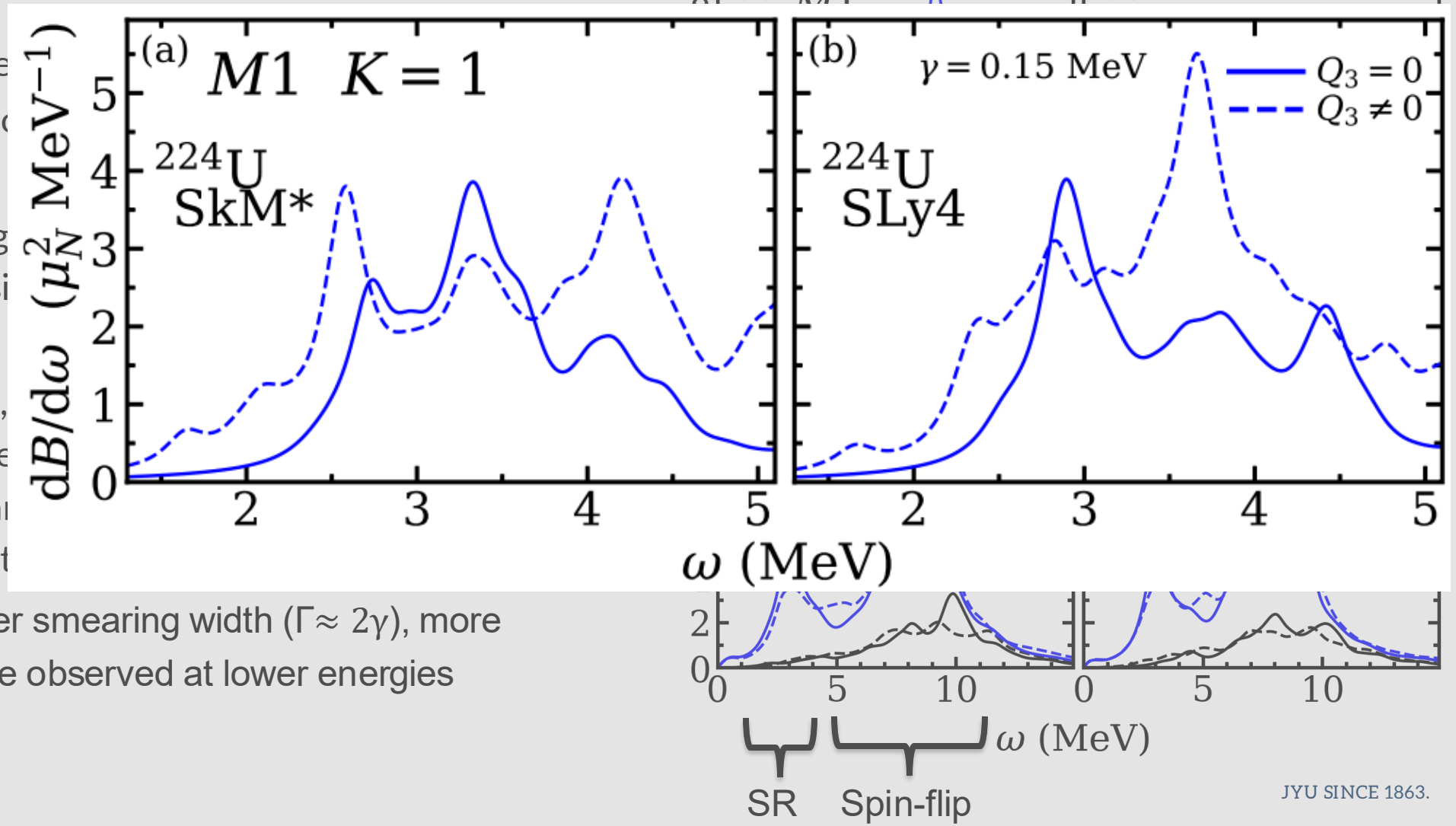

Magnetic dipole response – sum rules

- Non-energy-weighted sum rule m_0 for low-energy transitions (0–5 MeV) in all studied nuclei with A = 222–230
- m_0 is expected to scale linearly with the moment of inertia
  - This trend is observed for both deformation minima (panels a–c)
  - Octupole-deformed solutions are concentrated at the upper end of the moment-of-inertia range
    → correspondingly larger m_0 values
- m_0 is also expected to scale with ${\beta_2}^2$
  - This correlation is weakened for octupole-deformed solutions (panels d–f)
    → could serve as a signature of octupole deformation in experiments

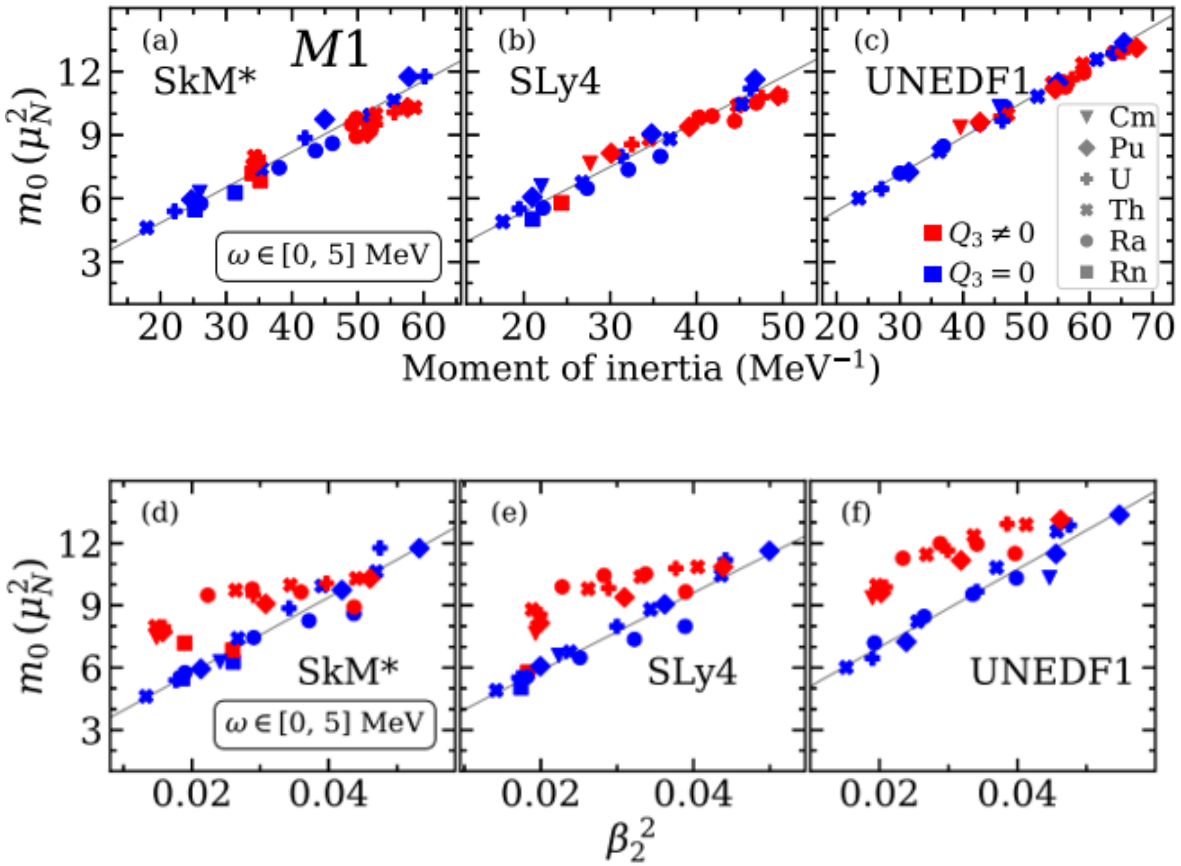

Electric quadrupole response

- Isoscalar (IS) and isovector (IV) *E*2 strength functions for ^{226}Ra calculated with the SkM* functional
  - The rotational spurious mode is removed in the IS *K*=1 channel
- Octupole deformation has little effect at resonance energies
- Differences appear at low energies (IS), which can be related to changes in the potential energy surface between the two deformation minima

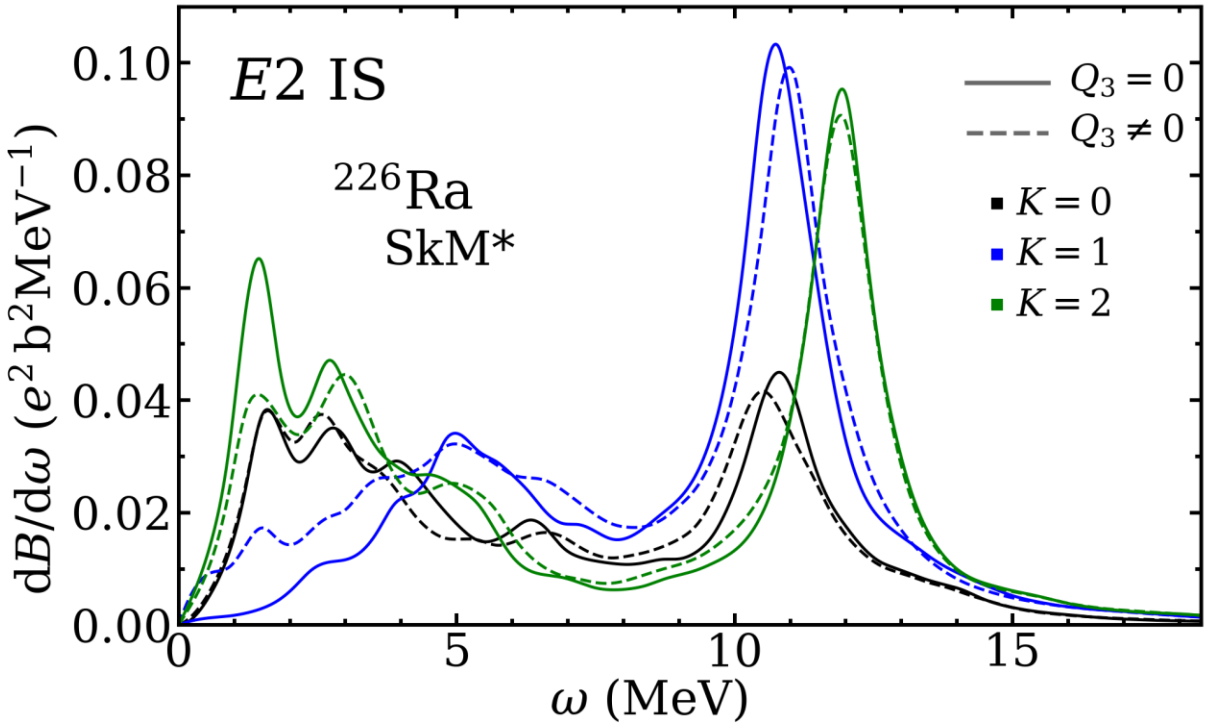

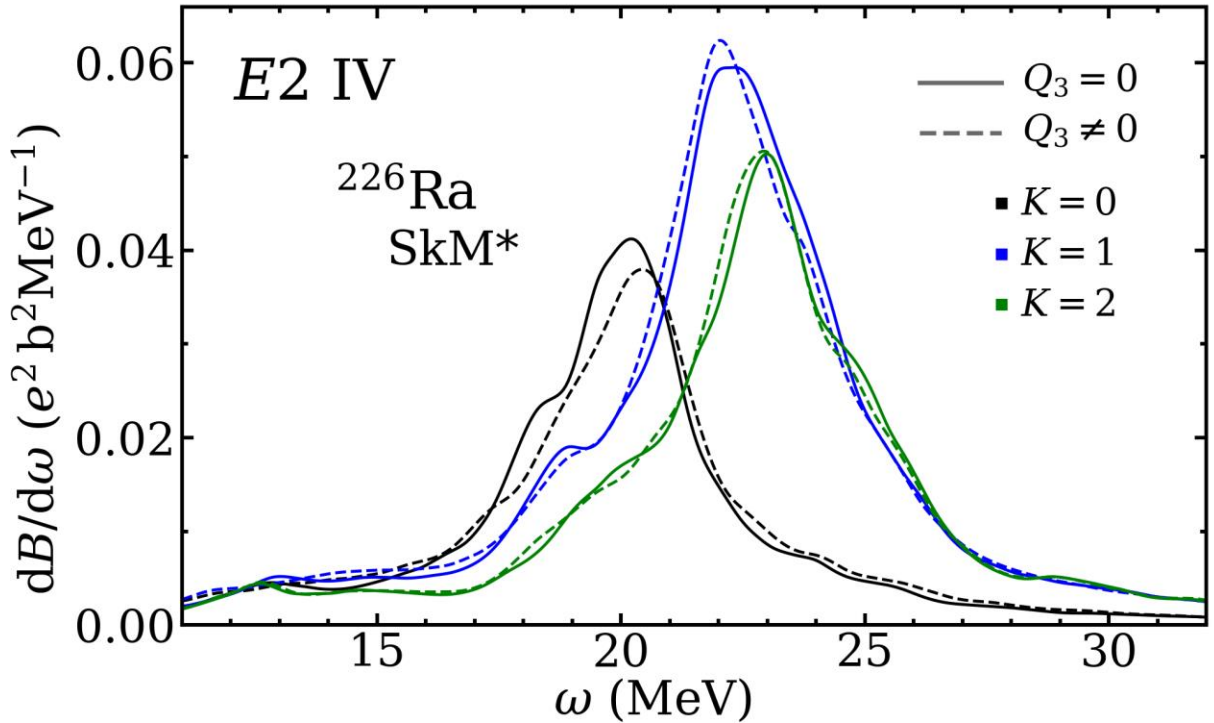

Electric octupole response – rotational spurious mode

- Isoscalar *E*3 transition strength function calculated using **three different treatments of spurious contributions:**
  1. no removal
  2. removal of linear mode only
  3. removal of both linear and rotational modes
- The octupole-deformed solution exhibits a significant rotational spurious component due to broken parity symmetry
- This contribution must be removed in the IS *E*3 *K*=1 channel to obtain a physical strength distribution

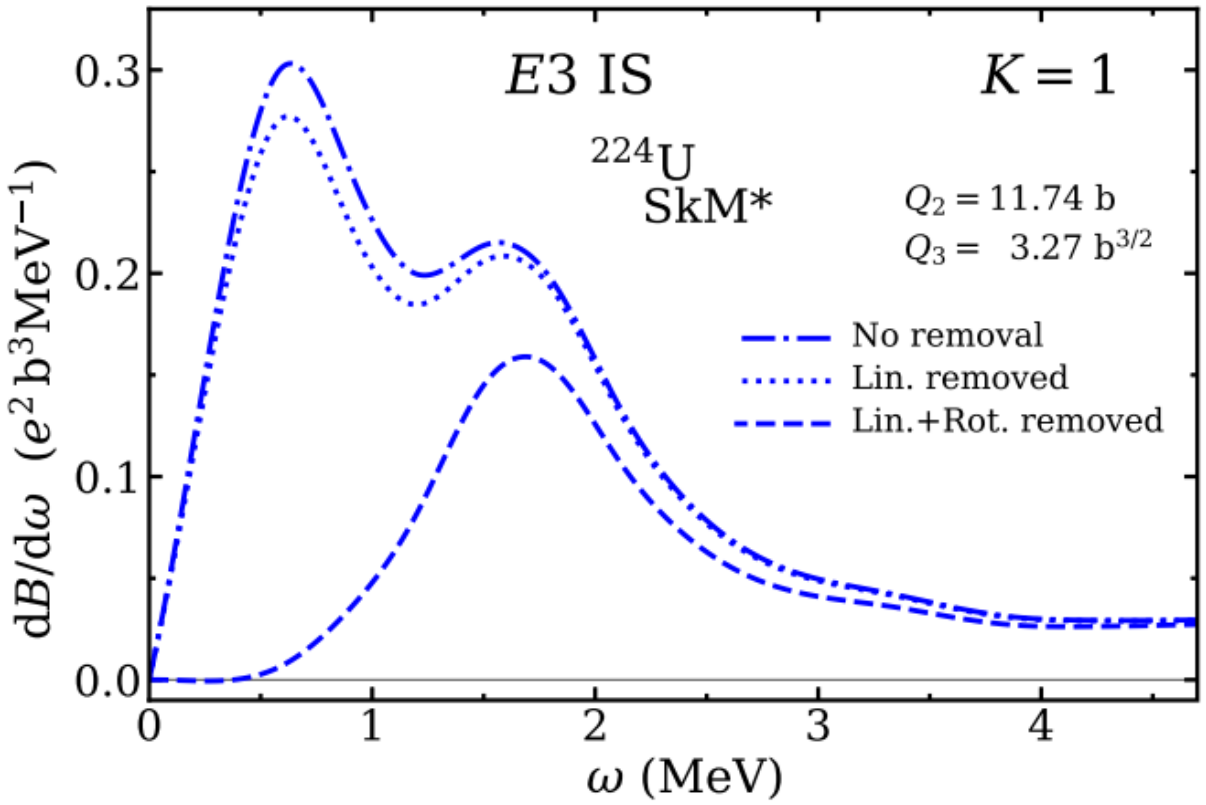

Electric octupole response

- Isoscalar and isovector *E*3 strength functions for ^{226}Ra calculated with the SkM* functional
  - All relevant linear and rotational spurious contributions are removed in the *K*=0 and *K*=1 channels
- At resonance energies, octupole deformation has little effect on the strength distributions
- Differences appear at low energies in the IS channel
  - Again, these can be related to changes in the potential energy surfaces around the two deformation minima

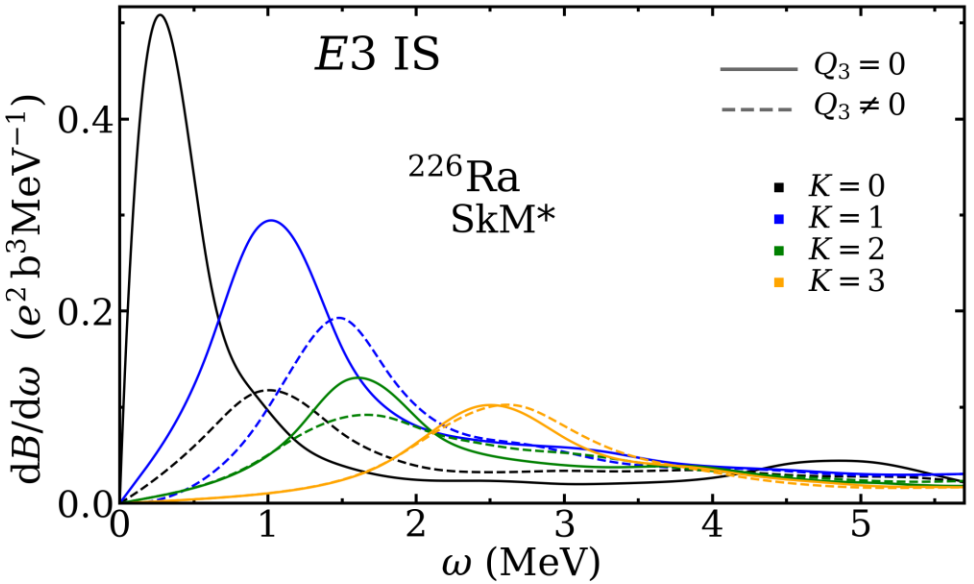

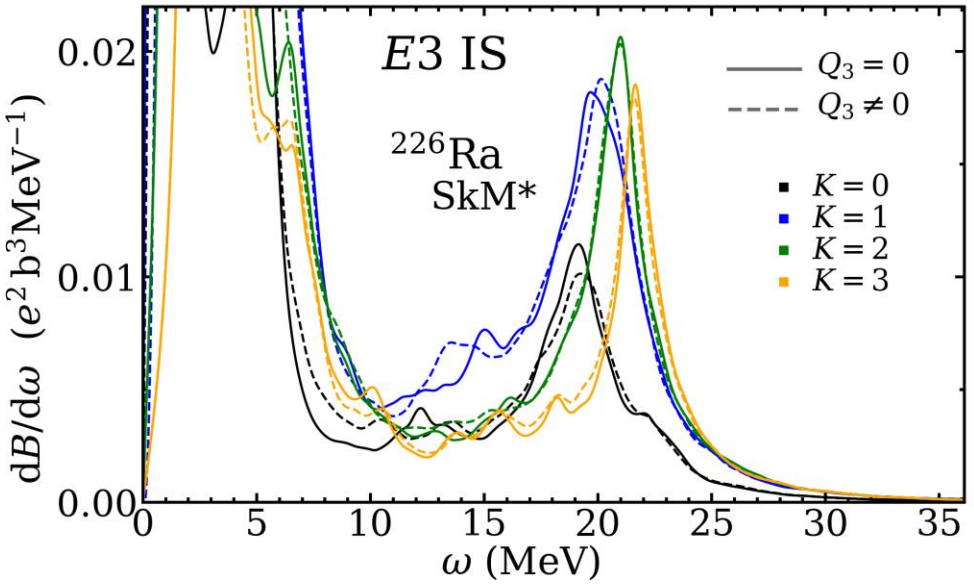

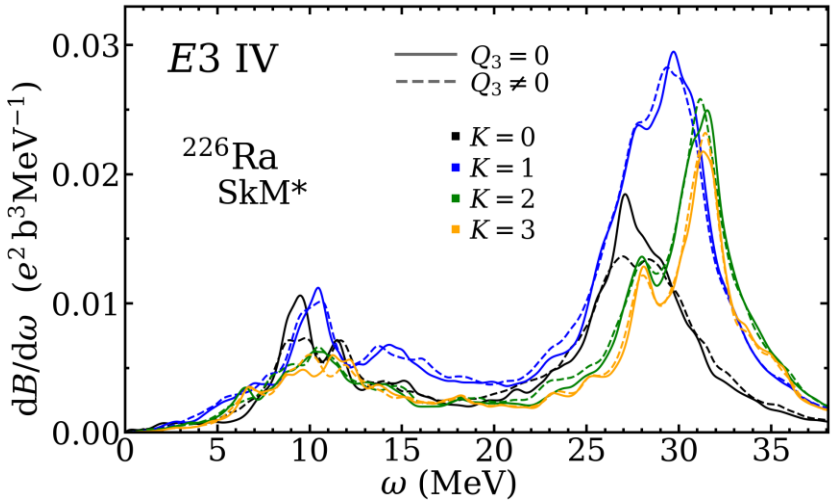

Conclusions

- **Octupole deformation** has a limited effect at resonance energies across all multipole modes
- **Low-energy M1 response** shows differences in strength distributions and total strength
- In parity-broken solutions, the rotational spurious mode must also be removed in the $K = 1^-$ channel (e.g., isoscalar E3)
- Observed trends are consistent across Skyrme functionals

Outlook

- Open question: role of parity (and rotational) symmetry restoration
- Low-energy M1 excitation modes
  - → Detailed role of octupole deformation in individual M1 modes
  - → May provide an experimental signature of octupole deformation

Electromagnetic response of A = 288–290 isotopes

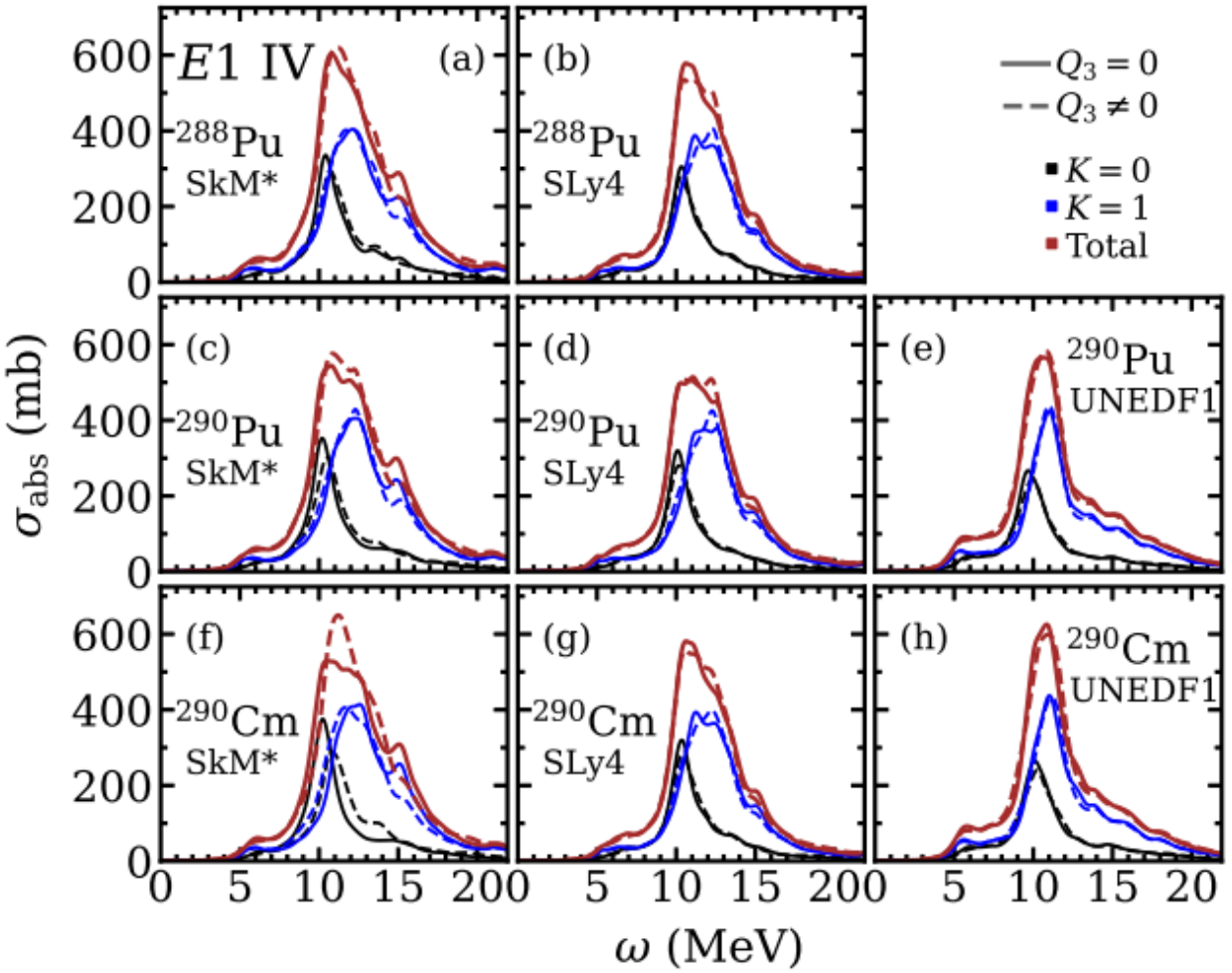

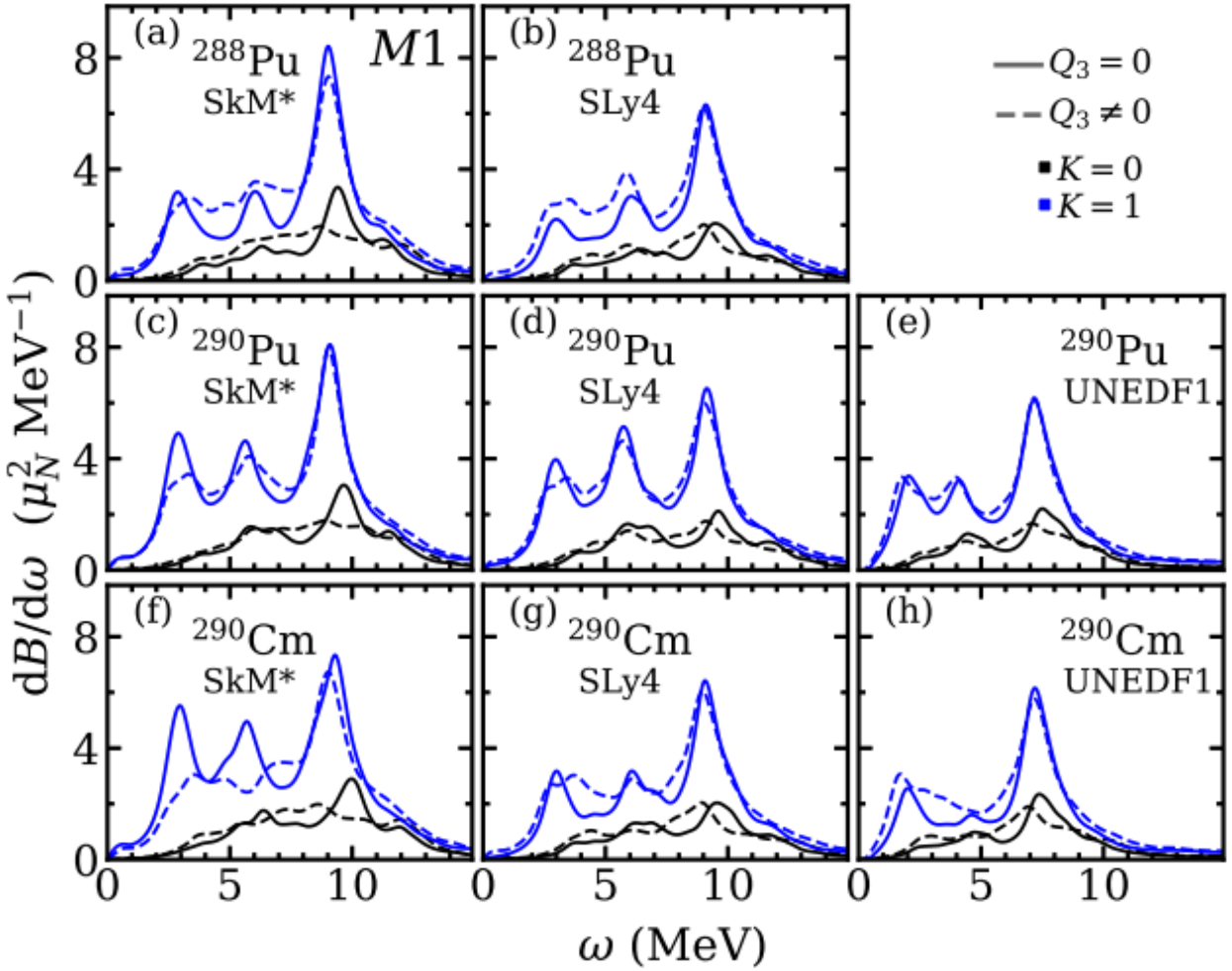

Magnetic dipole response in Th isotopes (SkM*, SLy4, UNEDF1)

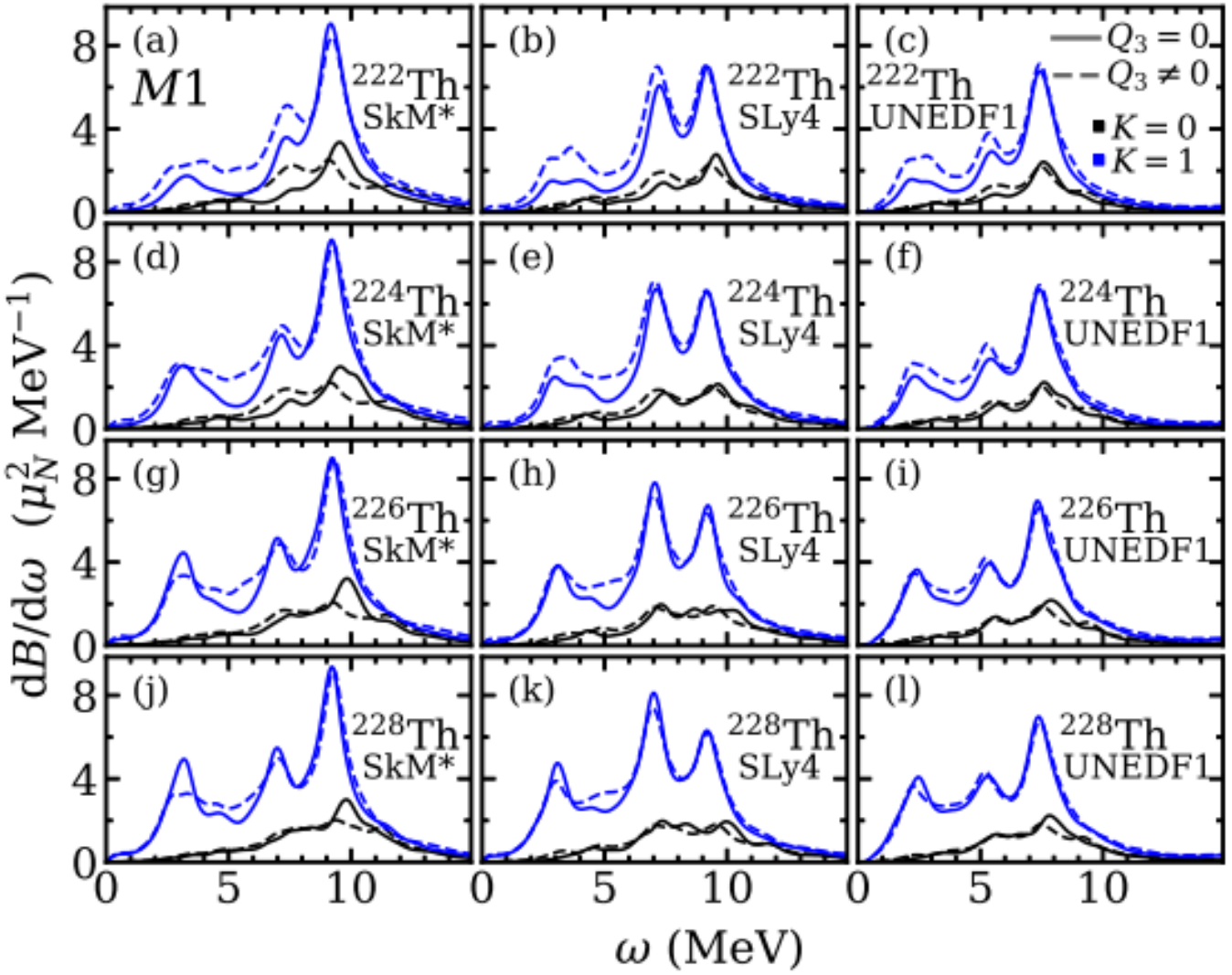

Magnetic dipole response – impact of Landau parameter

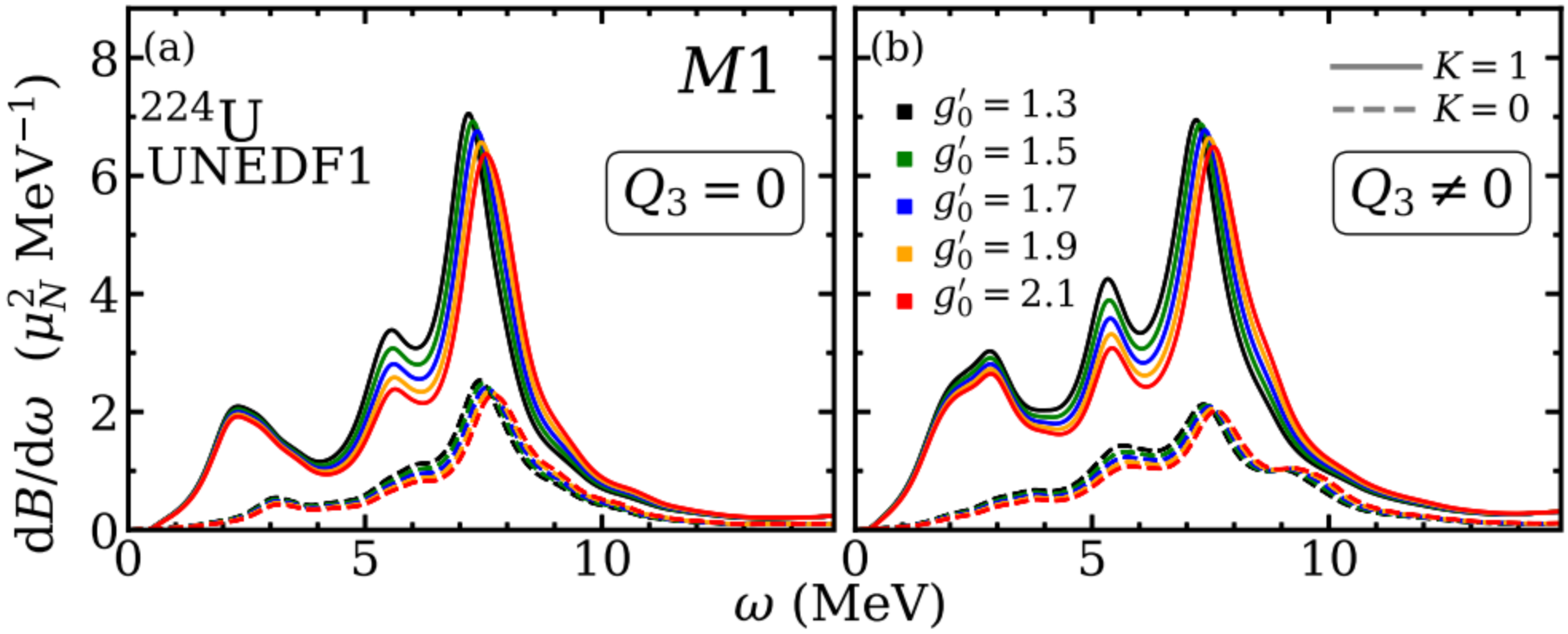

Magnetic dipole response – energy-weighted sum rules

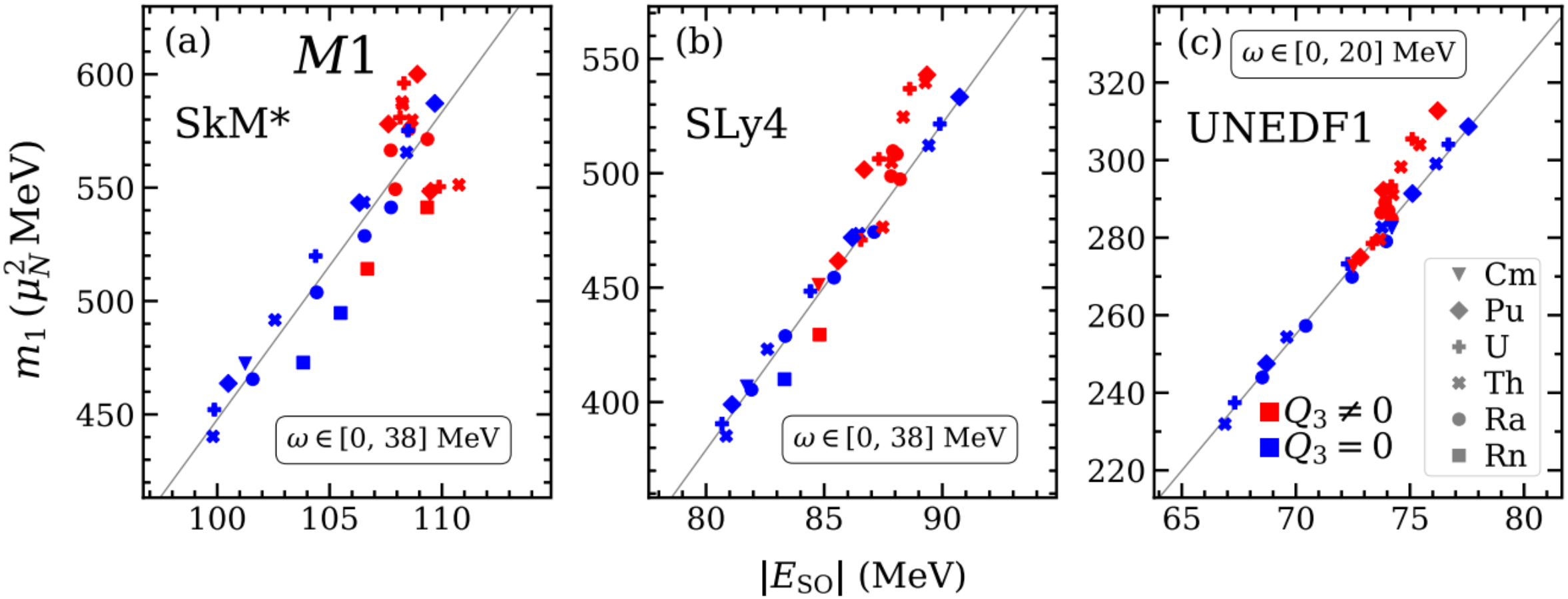

Electric quadrupole response (IS and IV) in Ra isotopes

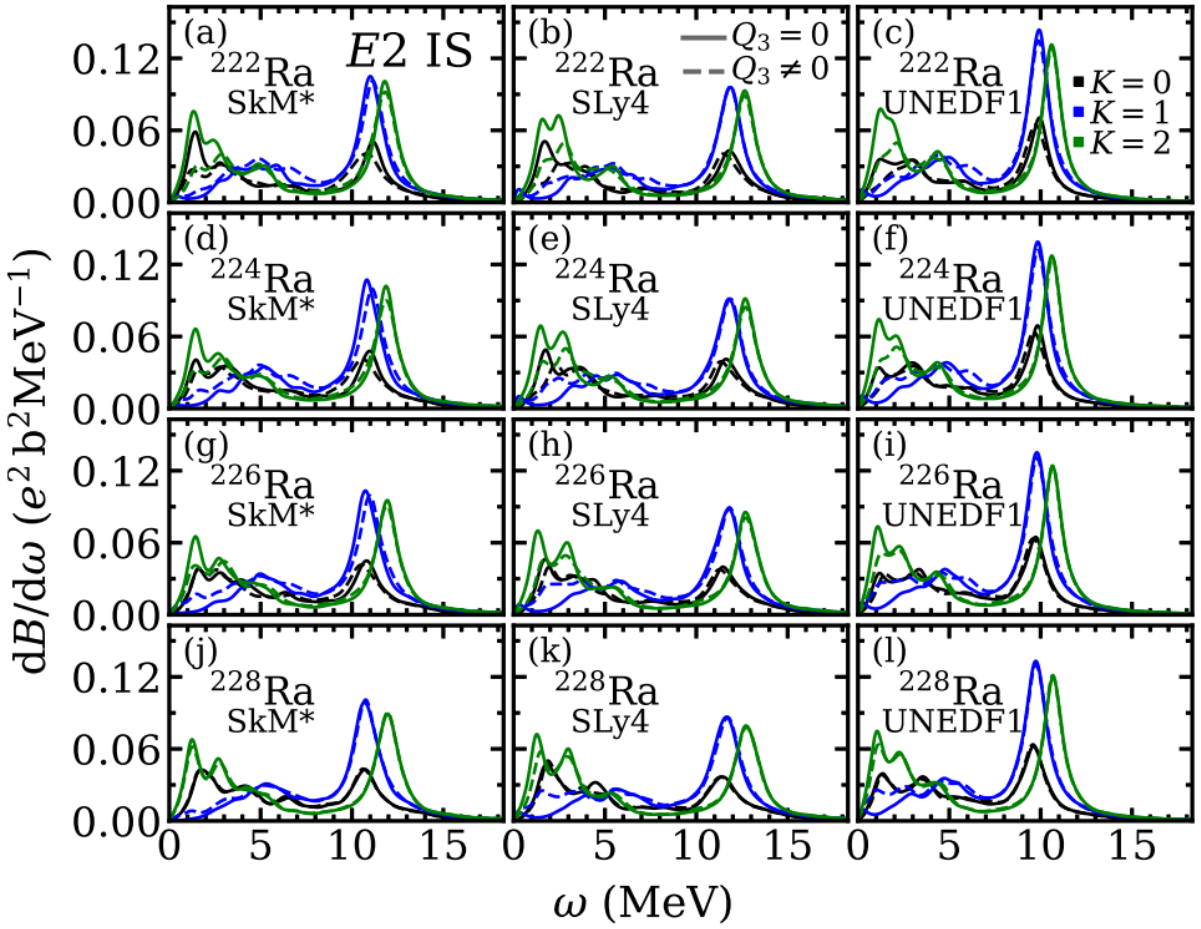

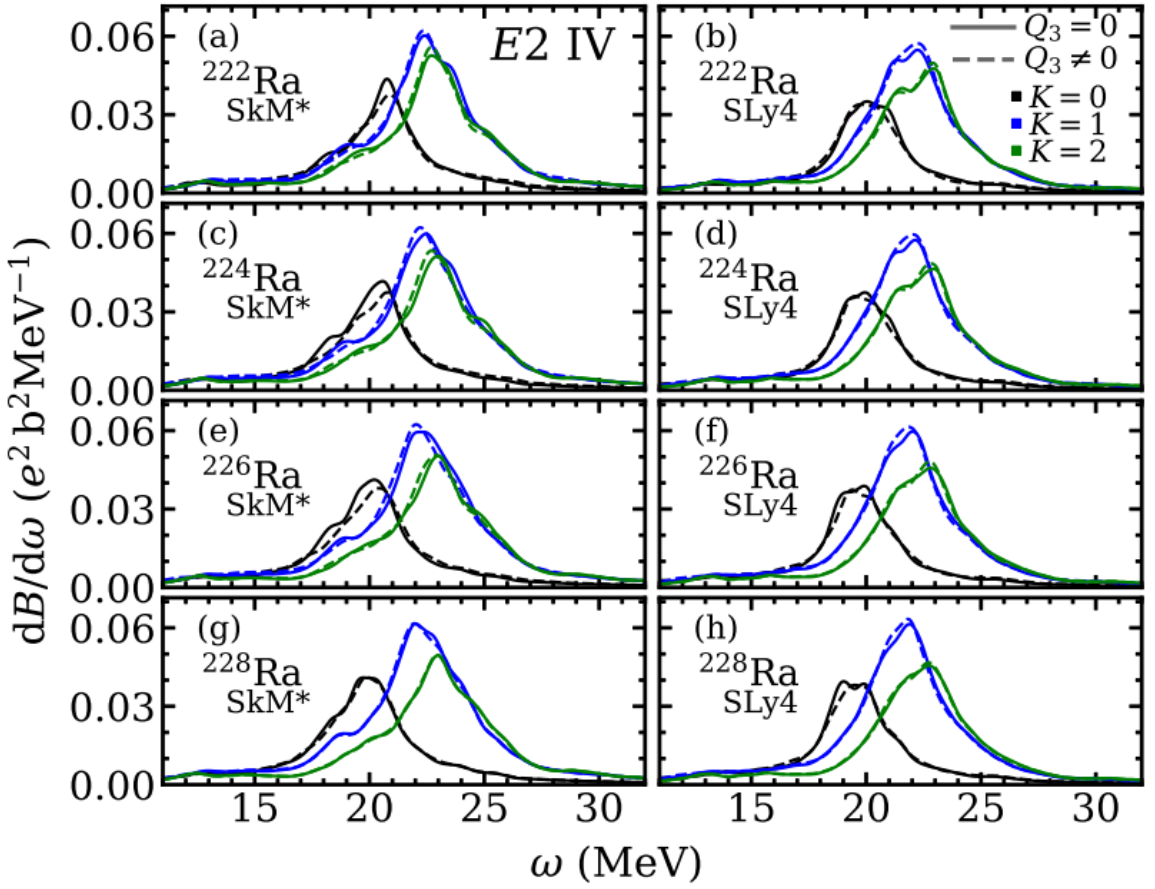

Electric octupole response (IS and IV) in Ra isotopes

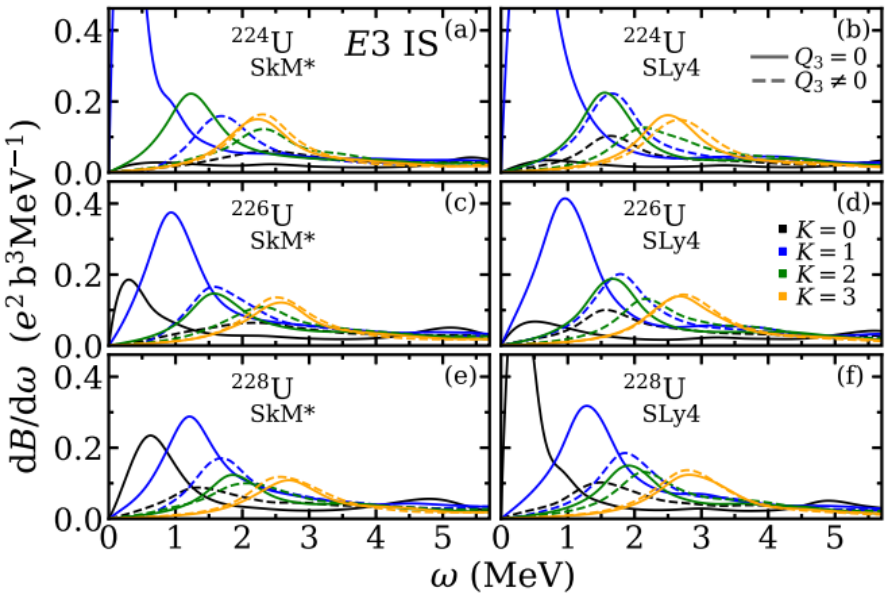

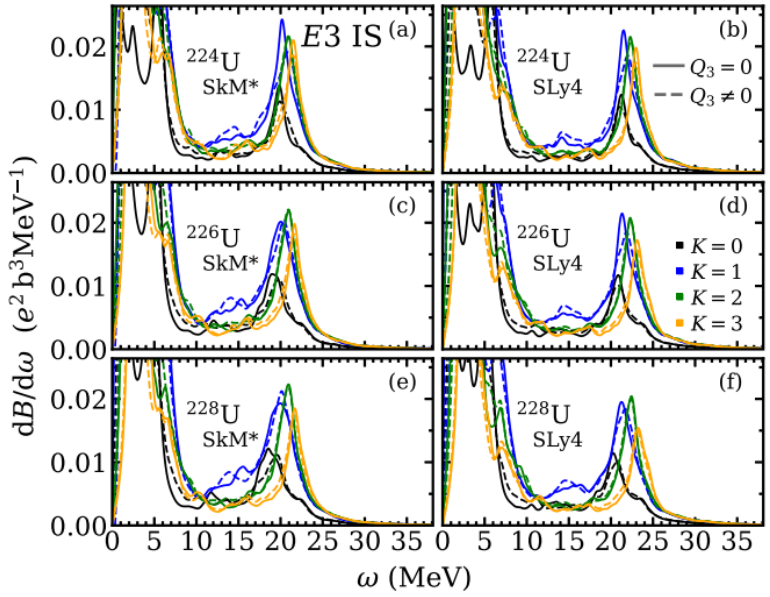

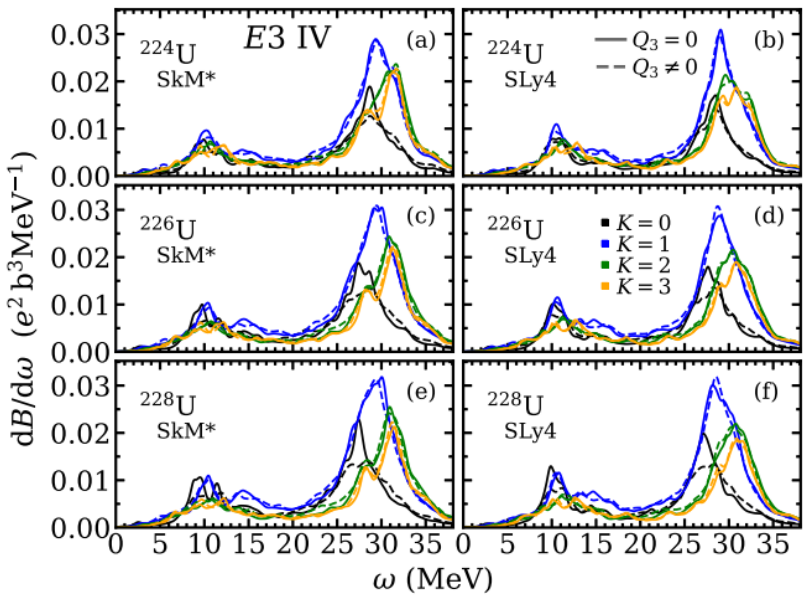

Ground state properties

Nucleus	Force	Q_2' (b)	Q_2 (b)	Q_3 (b$^{3/2}$)	$E(Q_2',0)$ (MeV)	$E_{\rm def}(0,0)$ (MeV)	$E_{\rm def}(Q_2,Q_3)$ (MeV)
^{222}Rn	SkM*	12.509	12.669	2.830	-1703.679	0.595	-0.438
	SLy4	12.112	12.427	1.127	-1699.971	1.197	-0.027
^{224}Rn	SkM*	15.075	15.082	1.792	-1714.463	1.690	-0.053
^{222}Ra	SkM*	12.615	13.780	3.311	-1701.435	0.807	-1.391
	SLy4	12.363	13.920	2.484	-1701.029	1.301	-0.700
	UNEDF1	12.773	14.133	2.435	-1707.339	1.329	-0.611
^{224}Ra	SkM*	15.922	15.953	3.395	-1713.749	2.351	-0.919
	SLy4	14.809	15.788	2.707	-1711.932	2.599	-0.659
	UNEDF1	15.245	15.972	2.556	-1718.647	2.417	-0.511
^{226}Ra	SkM*	18.343	18.121	2.988	-1725.840	3.946	-0.322
	SLy4	17.093	17.546	2.644	-1722.532	3.881	-0.423
	UNEDF1	17.476	17.683	2.262	-1729.661	3.504	-0.266
^{228}Ra	SkM*	20.257	20.282	1.409	-1737.544	5.282	-0.026
	SLy4	19.107	19.162	2.044	-1732.786	5.082	-0.129
	UNEDF1	19.399	19.378	1.617	-1740.286	4.484	-0.070
^{222}Th	SkM*	10.521	11.125	3.106	-1695.131	0.218	-1.619
	SLy4	10.879	12.626	2.398	-1697.522	0.527	-0.717
	UNEDF1	11.292	12.888	2.453	-1703.599	0.563	-0.821
^{224}Th	SkM*	15.239	15.242	3.559	-1708.708	1.944	-1.522
	SLy4	14.393	15.174	2.839	-1709.960	2.138	-0.943
	UNEDF1	14.934	15.387	2.872	-1716.354	1.907	-0.979
^{226}Th	SkM*	18.802	17.734	3.620	-1722.446	4.117	-0.783
	SLy4	17.635	17.376	3.115	-1722.243	3.690	-0.757
	UNEDF1	18.340	17.566	3.084	-1728.973	3.428	-0.714
^{228}Th	SkM*	21.004	20.406	3.090	-1735.774	6.036	-0.163
	SLy4	20.245	19.578	3.113	-1734.235	5.437	-0.348
	UNEDF1	20.783	19.797	2.962	-1741.264	4.739	-0.266

Nucleus	Force	Q_2' (b)	Q_2 (b)	Q_3 (b$^{3/2}$)	$E(Q_2',0)$ (MeV)	$E_{\rm def}(0,0)$ (MeV)	$E_{\rm def}(Q_2,Q_3)$ (MeV)
^{224}U	SkM*	12.347	11.741	3.271	-1699.625	0.811	-1.648
	SLy4	12.173	13.171	2.596	-1703.603	0.735	-0.773
	UNEDF1	12.831	13.504	2.752	-1709.794	0.786	-1.009
^{226}U	SkM*	17.556	16.236	3.692	-1714.514	2.969	-1.256
	SLy4	16.423	16.185	3.059	-1717.310	2.687	-0.853
	UNEDF1	17.570	16.504	3.185	-1723.823	2.427	-0.989
^{228}U	SkM*	21.106	19.360	3.678	-1729.555	5.555	-0.366
	SLy4	20.363	18.854	3.345	-1730.966	4.905	-0.502
	UNEDF1	21.163	19.103	3.415	-1737.786	4.377	-0.528
^{226}Pu	SkM*	13.774	11.869	3.402	-1702.691	1.161	-1.519
	SLy4	13.336	13.369	2.692	-1708.162	0.944	-0.659
	UNEDF1	14.632	13.510	2.950	-1714.458	1.036	-0.960
^{228}Pu	SkM*	19.776	16.988	3.725	-1718.772	3.698	-0.834
	SLy4	18.371	17.025	3.076	-1723.076	3.198	-0.539
	UNEDF1	20.685	17.291	3.302	-1729.784	3.118	-0.601
^{230}Pu	SkM*	22.713	21.176	3.371	-1734.851	6.607	-0.043
	SLy4	22.001	20.666	3.099	-1737.920	5.705	-0.165
	UNEDF1	23.101	21.265	3.228	-1744.877	5.359	-0.134
^{288}Pu	SkM*	20.266	15.931	5.402	-1992.829	0.190	-1.438
	SLy4	17.218	18.117	4.589	-1952.142	0.005	-0.849
^{290}Pu	SkM*	28.325	22.099	5.798	-1997.272	1.956	-0.509
	SLy4	25.124	22.511	5.050	-1954.144	1.488	-0.569
	UNEDF1	23.298	20.739	4.605	-1980.658	0.249	-0.796
^{228}Cm	SkM*	14.887	11.699	3.513	-1704.331	1.456	-1.326
	SLy4	14.345	13.373	2.708	-1711.228	1.267	-0.457
	UNEDF1	20.438	13.273	3.138	-1717.665	1.424	-0.736
^{290}Cm	SkM*	32.332	13.996	5.551	-2015.804	0.860	-1.316
	SLy4	19.380	17.595	4.897	-1978.145	0.450	-0.910
	UNEDF1	16.680	15.428	4.605	-2002.682	0.224	-1.240